Materials Science-Poland, Vol. 22, No. 4, 2004

Quantum networks in the presence of the Rashba effect and a magnetic field

DARIO BERCIOUX[1*], MICHELE GOVERNALE[2],
VITTORIO CATAUDELLA[1], VINCENZO MARIGLIANO RAMAGLIA[1]

[1]Coherentia-INFM and Dipartimento di Scienze Fisiche Università degli studi Federico II,
I-80126 Napoli, Italy

[2]NEST-INFM and Scuola Normale Superiore, Piazza dei Cavalieri 7, I-56126 Pisa, Italy

We use a simple formalism to calculate the conductance of any quantum network consisting of single-channel one-dimensional quantum wires in the presence of Rashba spin-orbit coupling and a coupling magnetic field. We show that the Rashba effect may give rise to an electron localization phenomenon similar to the Aharonov–Bohm effect. This localization effect can be attributed to spin precession due to the Rashba effect. We present results for linear transport through a finite-size chain connected to leads, taking also the effect of disorder into account. The effects of applying a magnetic field and Rashba spin-orbit coupling are studied in two-dimensional networks, showing that their interplay can lead the system to a transition between localized and anti-localized behaviour.

Key words: *Rashba effect; quantum networks; Aharonov–Bohm effect; localization*

1. Introduction

In the recent years, a new effect of extreme localization in a large class of rhombus tiling networks has been discussed [1]. This effect is related to an interplay between the Aharonov–Bohm (AB) effect [2] and geometry of the network. Actually, for particular values of the magnetic field, the set of sites visited by an initially localized wave packet is bound by the AB destructive interference. This set of sites is referred to as the AB cage. Such a localization does not rely on disorder [3], but only on quantum-interference and on the geometry of the lattice. There have been several theoretical papers addressing different aspects of AB cages, such as the effect of disorder and electron–electron interaction [4], interaction-induced delocalisation [5], and trans-

[*]Corresponding author, e-mail: dario.bercioux@na.infn.it. Present address: Institut für Theoretische Physik, Universität Regensburg, D-93040, Germany.

port [6]. From the experimental point of view, the AB-cage effect has been demonstrated for superconducting [7] and metallic networks [8] in the so-called T_3 lattice.

It is known that the wave function on an electron moving in the presence of spin-orbit (SO) coupling acquires quantum phases due to the Aharonov–Casher effect [9–14]. We focus on the Rashba SO coupling [15, 16], present in semiconductor heterostructures due to the lack of inversion symmetry in the growth direction. It is usually important in small-gap zinc-blende type semiconductors, and its strength can be tuned by external gate voltages. This has been demonstrated experimentally by measuring Shubnikov–de Haas oscillations in two-dimensional electron gas (2DEG) [17–19].

In the recent letter [20], we have shown that it is possible to obtain a localization of the electron wave function by means of the Rashba effect in quantum networks with a particular bipartite geometry containing nodes with different coordination numbers. This phenomenon has been demonstrated for a linear chain of square loops connected at one vertex (Fig. 1), which has been termed the diamond chain.

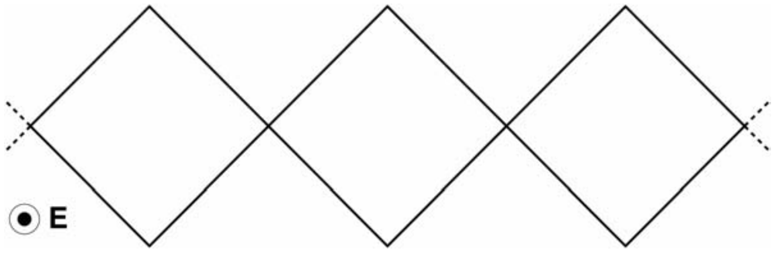

Fig. 1. Schematic view of the diamond chain

In this paper, the formalism introduced in our previous work [20] is improved in order to take into account the phase factor due to the magnetic field. The mechanism of electron localization owing to Rashba an SO coupling is analysed and compared in detail with the AB effect. It is shown that electron localization caused by the Rashba SO coupling is achieved only in geometrical structures that satisfy particular restrictions. Furthermore, we study the effect of applying SO coupling and a magnetic field on the transport properties of two different two-dimensional structures, the T_3 and square networks. One of the main results shown here is that a combination of both effects induces the phenomenon of electron anti-localization.

The paper is organized in the following way. In the Section 2 we introduce a very general formalism for studying quantum networks, realized with single-channel quantum wires in the presence of Rashba SO coupling and an external magnetic field. Section 3 is devoted to the transport properties of the diamond chain in presence of Rashba SO coupling alone. A physical interpretation of the localization phenomena due to Rashba SO coupling and a magnetic field is presented in Section 4. Section 5 is devoted to two different kinds of two-dimensional quantum networks in presence of Rashba SO coupling and a magnetic field. The paper ends with short conclusions of the presented results.

2. Model and formalism

We consider a single-channel quantum wire in a generic direction $\hat{\gamma}$ in the plane (x,y). The system is in the presence of a magnetic field B perpendicular to the plane (x,y) and Rashba SO coupling. The Hamiltonian for the single-channel quantum wire is:

$$H = \frac{\left(\vec{p} + q\vec{A}\right)^2}{2m} + \frac{\hbar k_{\mathrm{SO}}}{m}\left[\vec{\sigma} \times \left(\vec{p} + q\vec{A}\right)\right] \cdot \hat{z} + V(\hat{\gamma}) \tag{1}$$

where m is the electron mass, $\vec{A}$ is the vector potential relative to the magnetic field ($\vec{B} = \vec{\nabla} \times \vec{A}$), k_{SO} is the SO coupling strength and $V(\hat{\gamma})$ is the wire confining potential. The SO coupling strength k_{SO} is related to the spin precession length L_{SO} by the relation $L_{\mathrm{SO}} = \pi/k_{\mathrm{SO}}$. For InAs quantum wells, the spin-precession length ranges from 0.2 to 1 μm [17–19]. The wave function on a bond (quantum wire) connecting nodes α and β, in the direction $\hat{\gamma}_{\alpha\beta}$, which takes into account SO coupling and the magnetic field, is

$$\Psi_{\alpha\beta}(r) = \frac{\mathrm{e}^{-if_{\alpha r}}\mathrm{e}^{i(\vec{\sigma}\times\hat{z})\cdot\hat{\gamma}_{\alpha\beta}k_{\mathrm{SO}}r}}{\sin(kl_{\alpha\beta})}\left\{\sin\left[k(l_{\alpha\beta} - r)\right]\Psi_\alpha + \sin(kr)\mathrm{e}^{if_{\alpha\beta}}\mathrm{e}^{-i(\vec{\sigma}\times\hat{z})\cdot\hat{\gamma}_{\alpha\beta}k_{\mathrm{SO}}l_{\alpha\beta}}\Psi_\beta\right\} \tag{2}$$

where k is related to the eigenenergy by $\varepsilon = \left(\hbar^2/2m\right)(k^2 - k_{\mathrm{SO}}^2)$*, r is the coordinate along the bond, and $l_{\alpha,\beta}$ is the length of the bond. The spinors Ψ_α and Ψ_β are the values of the wave function at the nodes α and β, respectively. Spin precession due to the Rashba effect is described by the exponentials containing Pauli matrices in Eq. (2). The magnetic field contributes through the phase factor of the wave function (2)

$$\exp\left\{-if_{\alpha,r}\right\} = \exp\left\{-i\frac{2\pi}{\phi_0}\int_\alpha^r \vec{A}\cdot d\vec{l}\right\} \tag{3}$$

where $\phi_0 = h/e$ is the flux quantum.

The wave function of the whole network [6, 20, 21] is obtained by imposing the continuity of probability current at the nodes. For a generic node α, it reads:

$$\mathbf{M}_{\alpha\alpha}\Psi_\alpha + \sum_{<\alpha,\beta>} \mathbf{M}_{\alpha\beta}\Psi_\beta = 0 \tag{4}$$

where

$$\mathbf{M}_{\alpha\alpha} = \sum_{<\alpha,\beta>} \cot kl_{\alpha\beta} \quad \text{and} \quad \mathbf{M}_{\alpha\beta} = -\frac{\mathrm{e}^{-if_{\alpha\beta}}\mathrm{e}^{-i(\vec{\sigma}\times\hat{z})\cdot\hat{\gamma}_{\alpha\beta}k_{\mathrm{SO}}l_{\alpha\beta}}}{\sin kl_{\alpha\beta}} \tag{5}$$

In Eqs. (4), (5), the sum $\sum_{<\alpha,\beta>}$ runs over all nodes β connected by bonds tothe node α.

---

* The term in k_{SO}^2 can be neglected in realistic situations.

3. The one-dimensional case

The one-dimensional analysis takes into account the case where only SO coupling is present, that is the magnetic field is zero ($B = 0$) [20].

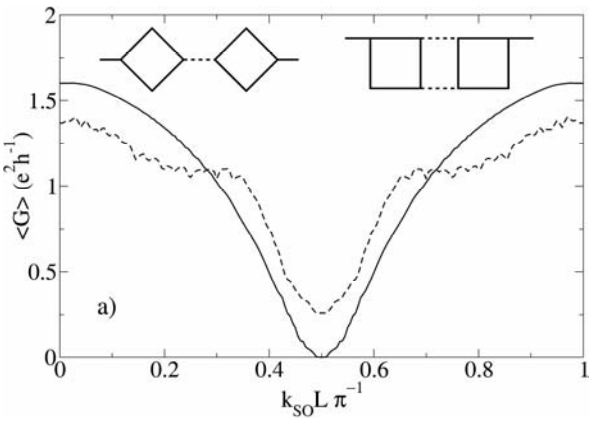

Fig. 2. Conductance (averaged over k_{in}) as a function of spin-orbit coupling strength for the diamond chain (continuous line) and for the ladder (dashed line). The two finite-size systems connected to input/output leads are shown in the inset. The parameters used for the calculation are: 50-elementary loops, k_{in} uniformly distributed in $[0, \pi/L]$

In the case of the AB cage, the first experimental verification came from transport measurements [7, 8]. To propose a possible experimental verification of the Rashba -cage effect, we evaluate the linear conductance of a diamond chain of finite length. To show that the localization effect is due to the peculiar bipartite geometry of the lattice, containing nodes with different coordination numbers, we contrast the diamond chain with a square ladder, i.e. a chain of square loops connected at two vertices, (the inset of Fig. 2). In the following, we will also refer to the latter topology simply as the ladder. The formalism to study the transport properties in the ladder has been introduced in the Ref. [20].

For a given k_{in}, the conductance has a rich structure, which takes into account the complexity of the associated energy spectrum [20]. In particular, on increasing k_{SO} gaps open and the energy of the incoming electrons ($\varepsilon_{in} = (\hbar^2 k_{in}^2 / 2m)$) can enter one of these gaps, leading to a vanishing conductance but not to a localization [20]. In fact, in this case the insulating behaviour is due to the absence of available states at the injection energy and not to the localization of the electron wave function in space. This effect is not present in $< G(k_{SO} L) > k_{in}$, since integration over k_{in} is equivalent to an average over energy. The dependence of the average conductance $< G(k_{SO} L) >_{k_{in}}$ on k_{SO} is shown in Fig. 2 for both the diamond chain and the square ladder. The conductance for both kinds of chains has a minimum for $k_{SO}L = \pi/2$, caused by phase differences induced by the Rashba effect. Due to the existence of the Rashba cages, however, this minimum reaches zero only for the diamond chain.

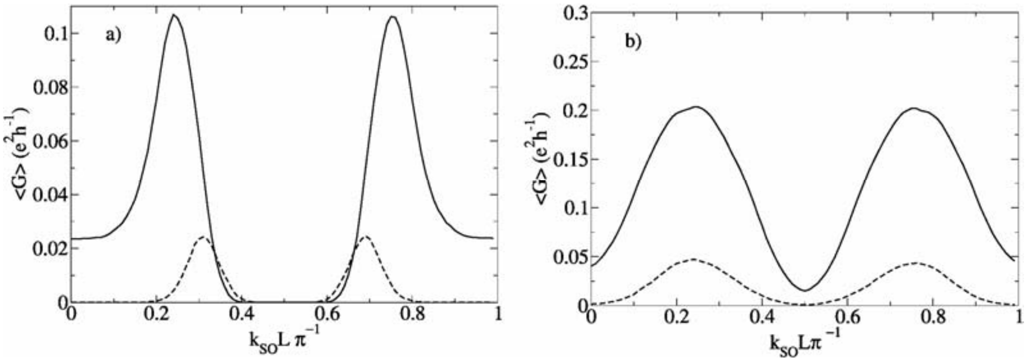

Fig. 3. Conductance (averaged over disorder configurations and over k_{in}) plotted as a function of spin-orbit coupling strength for the diamond chain (a) and the ladder (b). The two values of disorder strength used in the calculation were: $\Delta L = 0.01L$ (solid line) and $\Delta L = 0.02L$ (dashed line). Disorder averaging is done over 50 configurations, and k_{in} is uniformly distributed in $[k_F - \pi/2, k_F + \pi/2]$, with $k_F L = 100$. Both systems are composed of 50 elementary loops

From studies on AB cages, we expect the localization induced by the Rashba effect to be robust against disorder only in the bipartite structure that contains nodes with different coordination numbers (the diamond chain). A disorder that is more dangerous for the Rashba-cage effect is random fluctuation in the length of the bonds [6, 20], as such length fluctuations induce fluctuations in the phase shifts due to spin -precession. Hence, we consider a model where the length of each bond is randomly distributed in the interval $[L - \Delta L, L + \Delta L]$. The half width of the distribution ΔL gives the strength of the disorder.

In order to clarify if disorder affects the conductance, we average over disorder configurations. This is relevant to experiments, as in a real sample averaging is introduced by a finite phase-coherence length. For intermediate values of disorder ($k_F\Delta L \approx 1$), we find that the Rashba-cage effect is still present for the diamond chain, whereas the periodicity in k_{SO} is halved for the ladder, as shown in Fig. 3. The latter result can be interpreted as an analogue of the Altshuler–Aharonov–Spivak (AAS) effect [22] induced by the SO coupling. At higher values of disorder, the AAS effect also prevails in the diamond chain.

4. Physical interpretation

Let us consider the closed path in Fig. 4a, in which the four arms have the same length. An electron injected at the point A can reach the point D by moving through the upper path or though the lower path. The electron wave function gains a phase that depends on the Hamiltonian describing the travelled path. This corresponds to introducing a phase operator R_{pq} that relates the wave function at the starting point p with the its value in the end point q:

$$\psi(q) = R_{pq}\psi(p) \tag{6}$$

In this simple picture, the condition for having localization in this closed path is that an electron injected at the point A undergoes a destructive interference at D. This condition, in the mathematical form, corresponds to

$$(R_{BD} \cdot R_{AB} + R_{CD} \cdot R_{AC})\psi = 0, \quad \forall\, \psi \tag{7}$$

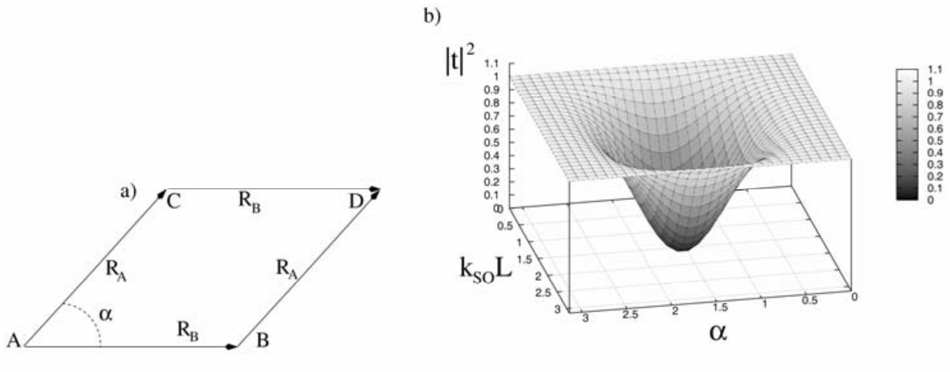

Fig. 4. Closed path between the points A and D (a). This is parameterised as a function of the angle α. Three-dimensional plot of the transmission probability as a function of the angle α between the paths AB and AC and spin-orbit coupling $k_{SO}L$ (b)

When Rashba SO coupling is present and the magnetic field is zero, the phase operator takes the spin precession into account being of the form

$$R_{pq} = \exp\left\{-i\int_p^q \vec{\sigma}\cdot\left(\hat{z}\times d\vec{l}\;\right)k_{SO}\right\} \tag{8}$$

i.e., this is a spin-dependent operator. From Eq. (7) it is possible to retrieve information about the transmission probability through the relation

$$|t|^2 = \mathrm{Tr}\left[\Gamma\Gamma^\dagger\right] \tag{9}$$

where $\Gamma = R_{BD} \cdot R_{AB} + R_{CD} \cdot R_{AC}$. In Figure 4b, the behaviour of the transmission probability (11) is shown as function of the angle α and of the SO coupling $k_{SO}L$. It is clear that the transmission probability goes to zero if and only if the angle between the path is equal to π/2 and SO coupling is equal to π/2. This implies that we can achieve a complete localization only in a linear chain of square loops connected at one vertex and not in a chain of rhombi.

When the magnetic field B is present and Rashba SO coupling is zero, the phase operator has the form

$$R_{pq} = \exp\left\{ -i \frac{2\pi}{\phi_0} \int_p^q \vec{A} d\vec{l} \right\} \tag{10}$$

This operator is strongly dependent on the path along which the electron travels and it does not depend on spin. If we replace this phase operator in Eq. (7), the solution of the localization problem is given by

$$B = \left(n + \frac{1}{2} \right) \frac{\phi_0}{\sin(\alpha) L^2} \tag{11}$$

This equation relates the magnetic field inversely to the area of the closed path and tells us that for each area it is possible to apply a magnetic field that induces electron localization [2].

5. The two-dimensional case

We now concentrate on a periodic tiling with the hexagonal symmetry, called T_3 (Fig 5a). This is a periodic hexagonal structure with three sites per a unit cell, one sixfold coordinated and two threefold coordinated. It is also an example of a two-dimensional regular bipartite lattice containing nodes with different coordination numbers.

In Figure 5b, the behaviour of the averaged conductance for a finite piece of the T_3 lattice is shown as a function of reduced flux with zero SO coupling and SO coupling with zero magnetic field. In the case of the magnetic field, we observe a suppression of conductance due to the existence of the AB cage. The value of the averaged conductance minimum is not exactly zero. This is due to the existence of dispersive edge states [6], which are able to carry current even for $\phi/\phi_0 = 1/2$. This value is independent of the number of injection channels.

In the case of SO coupling, we do not observe a strong suppression of the averaged conductance as in the case of the magnetic field. A minimum is present, but it is due to interference phenomena that do not induce complete localization. Furthermore, this minimum cannot be caused by the existence of edge states, because it depends on the number of injection channels.

In Figure 5c, the behaviour of the averaged conductance is shown as function of SO coupling with $\phi/\phi_0 = 1/2$ and the magnetic field with $k_{SO}L\pi^{-1} = 0.5$. In the first case, the averaged conductance starts out from a point of maximum localization due to the AB effect, in the second case the averaged conductance starts out from a point of maximum localization due to the Rashba SO coupling. The main feature of these two curves is that the general behaviour is similar in the case of fixed SO coupling as in the case without it. A well-defined minimum for $\phi/\phi_0 = 0.5$ is still observed. On the contrary, in the case of a fixed magnetic field we observe as the SO coupling suppress the destructive interference due to the AB effect and an anti-localization peak appears.

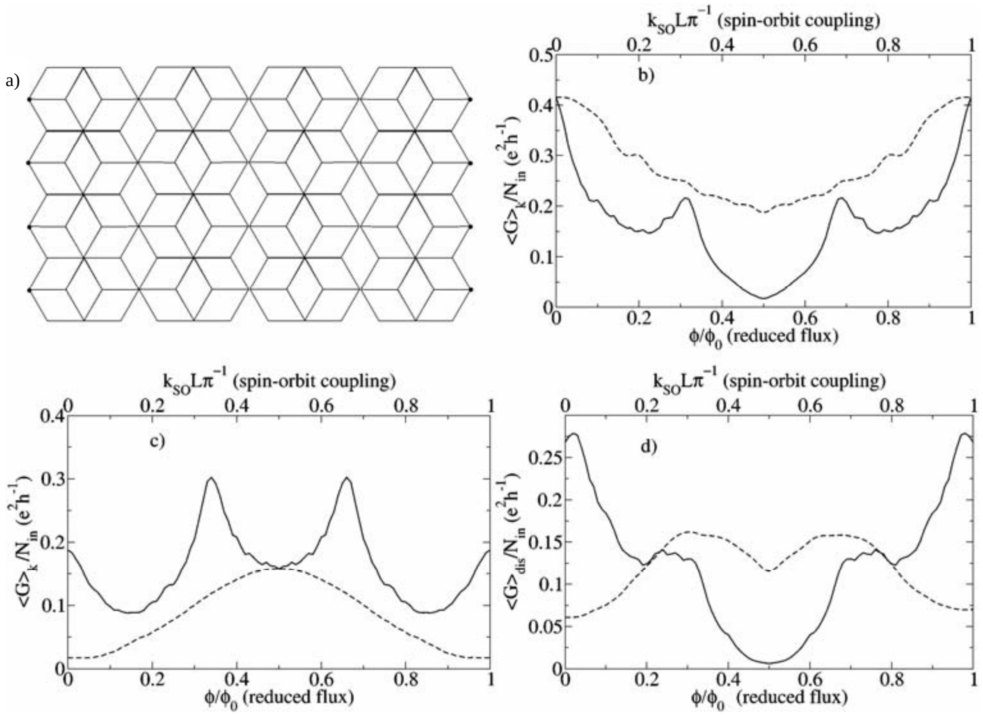

Fig. 5. A piece of the *T* network (a). Black dots on the left right) represent connections to the input (output) channels. Averaged conductance $<G>_{\boldsymbol{k}}/N_{in}$ as a function of reduced flux (solid curve) and spin-orbit coupling (dashed curve) for a T_3 lattice with 200 quantum wires (b). Averaged conductance $<G>_{\boldsymbol{k}}/N_{in}$ as a function of reduced flux evaluated at $k_{SO}L\pi^{-1} = 0.5$ (solid curve) and spin-orbit coupling evaluated at $\phi/\phi_0 = 0.5$ (dashed curve) for a T_3 lattice with 200 quantum wires (c). Averaged conductance $<G>_{dis}/N_{in}$ as function of reduced flux (solid curve) and spin-orbit coupling (dashed curve) for a T_3 lattice with 200 quantum wires in the disordered case (d)

In Figure 5d, the behaviour of the averaged conductance with respect to the disorder is shown as a function of reduced flux and SO coupling for a fixed disorder strength. It is clear that for the averaged conductance as a function of SO coupling the periodicity is no longer $k_{SO}L$, but $k_{SO}L/2$ according to the weak localization picture [22]. The averaged conductance as a function of reduced flux remains ϕ_0 periodic with a large amplitude. This strongly suggests that the AB cage effect survives for this strength of disorder.

We now consider transport through a finite square lattice (Fig. 6a). This network, unlike the T_3 lattice, does not present a bipartite structure containing nodes with different coordination numbers. Accordingly, we do not expect any electron localization phenomenon due to the AB effect or SO coupling. On the other hand, as we have shown in Section 4, the square network is composed of elementary cells (squares) that, as single elements, permit electron localization with both a magnetic field and SO coupling.

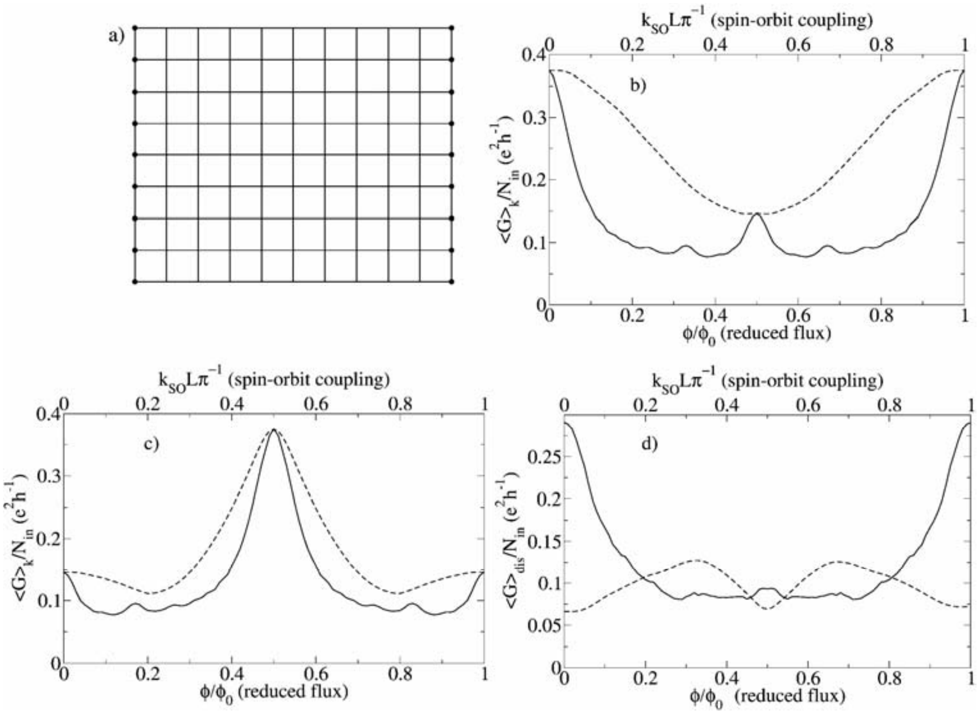

Fig. 6. A piece of the square lattice (a). Black dots on the left (right) represent the connections to the input (output) channels. Averaged conductance $<G>_{\boldsymbol{k}}/N_{in}$ as a function of reduced flux (solid curve) and spin-orbit coupling (dashed curve) for the square lattice with 178 quantum wires (b). Averaged conductance $<G>_{\boldsymbol{k}}/N_{in}$ as a function of reduced flux evaluated at $k_{SO}L\pi^{-1} = 0.5$ (solid curve) and spin-orbit coupling evaluated at $\phi/\phi_0 = 0.5$ (dashed curve) for the square lattice with 178 quantum wires (c). Averaged conductance $<G>_{dis}/N_{in}$ as a function of reduced flux (solid curve) and spin-orbit coupling (dashed curve) for the square lattice in the disordered case (d)

In Figure 6b, the behaviour of the averaged conductance for a finite piece of the square lattice is shown as a function of reduced flux with zero SO coupling and SO coupling with zero magnetic field. The behaviour of the averaged conductance in the case of SO coupling is completely different from that of the magnetic field. Both, however, reach the same value, the former for $k_{SO}L\pi^{-1} = 1/2$ and the latter for $\phi/\phi_0 = 1/2$. According to Section 4, both the AB effect and SO coupling induce electron localization in the elementary cell of the square network for these values, that is for these two critical values the system behaves the same way. If we now export this simple idea to the case of a square network, we infer that the conductance evaluated for $k_{SO}L\pi^{-1} = 1/2$ or $\phi/\phi_0 = 1/2$ has to show the same value.

It is interesting to analyse what happens when both the magnetic field and SO coupling are present. In Figure 6c, the behaviour of the averaged conductance is shown as a function of SO coupling with $\phi/\phi_0 = 1/2$ and the magnetic field with $k_{SO}L\pi^{-1} = 1/2$. The behaviour of both curves is very similar. The results of Section 4 tell us that these two localization phenomena manifest the same effect but as consequence of different physical aspects. In the case of SO coupling, we have a destructive interference between electrons undergoing spin-precession, instead of a spin-independent destructive interference process as in the case of the AB effect. When both localization phenomena are present at the maximum intensities, the destructive interference is completely lost. We then observe anti-localization rather than localization. The averaged conductance goes to the same value observed for zero magnetic field and zero SO coupling (Fig. 6b).

In Figure 6d, the behaviour of the averaged conductance is shown as a function of reduced flux and SO coupling in the case of a disordered system. It is also manifested in this case that the periodicity with respect to the magnetic flux and SO coupling is no longer ϕ_0 and $k_{SO}L$, but $\phi_0/2$ and $k_{SO}L/2$, respectively.

6. Conclusion

We have shown that in a quantum network with a particular bipartite geometry and containing nodes with different connectivities (a diamond chain), it is possible to obtain localization of the electron wave function by means of the Rashba effect. This localization shows up in the transport properties of a finite-size chain connected to leads. Furthermore, transport calculations in the presence of disorder show that this Rashba-cage effect is robust against disorder in the diamond chain. The effect of localization is not verified in two-dimensional networks with a bipartite structure and containing nodes with different coordination numbers, such as the T_3 lattice. We have shown, however, that the effect of applying Rashba SO coupling and a magnetic field can induce a strong anti-localization phenomena in those structures.

Acknowledgements

Fruitful discussion with C. Cacciapuoti, G. De Filippis, P. Lucignano and C.A. Perroni (Federico II University of Naples, Italy) and with R. Fazio, D. Frustaglia and M. Rizzi (Scuola Normale Superiore of Pisa, Italy) are gratefully acknowledged. Finally, DB wishes to acknowledge A. Ceré (Hippos Campi Flegrei of Naples, Italy).

References

[1] VIDAL J., MOSSERI R., DOUÇOT B., Phys. Rev. Lett., 81 (1998), 5888.
[2] AHARONOV Y., BOHM D., Phys. Rev., 115 (1959), 485.

[3] ANDERSON P.W., Phys. Rev., 109 (1958), 1492.
[4] VIDAL J., BUTAUD P., DOUÇOT B., MOSSERI R., Phys. Rev. B, 64 (2001), 155306.
[5] VIDAL J., DOUÇOT B., MOSSERI R., BUTAUD P., Phys. Rev. Lett., 85 (2000), 3906.
[6] VIDAL J., MONTAMBAUX G., DOUÇOT B., Phys. Rev. B, 62, R16294 (2000).
[7] ABILIO C.C., BUTAUD P., FOURNIER T., PANNETIER B., VIDAL J., TEDESCO S., DALZOTTO B., Phys. Rev. Lett., 83 (1999), 5102.
[8] NAUD C., FAINI G., MAILLY D., Phys. Rev. Lett., 86 (2001), 5104.
[9] AHARONOV Y., CASHER A., Phys. Rev. Lett., 53 (1984), 319.
[10] MATHUR H., DOUGLAS STONE A., Phys. Rev. Lett., 68 (1992), 2964.
[11] BALATSKY A.V., ALTSHULER B.L., Phys. Rev. Lett., 70 (1993), 1678.
[12] ARONOV A.G., LYANDA-GELLER Y.B., Phys. Rev. Lett., 70 (1993), 343.
[13] SPLETTSTÖßER J., GOVERNALE M., ZÜLICKE U., Phys. Rev. B, 68 (2003), 165341.
[14] FRUSTAGLIA D., RICHTER K., Phys. Rev. B, 69 (2004), 235310.
[15] RASHBA E.I., Fiz. Tverd. Tela (Leningrad), 2 (1960), 1224 (Sov. Phys. Solid State 2, 1109 (1960)).
[16] BYCHKOV Y.A., RASHBA E.I., J. Phys., C 17 (1984), 6039.
[17] NITTA J., AKAZAKI T., TAKAYANAGI H., ENOKI T., Phys. Rev. Lett., 78 (1997), 1335.
[18] SCHÄPERS T., ENGELS J., KLOCKE T., HOLLFELDER M., LÜTH H., J. Appl. Phys., 83 (1998), 4324.
[19] GRUNDLER D., Phys. Rev. Lett., 84 (2000), 2000.
[20] BERCIOUX D., GOVERNALE M., CATAUDELLA V., MARIGLIANO RAMAGLIA V., Phys. Rev. Lett., 93 (2004), 56802.
[21] KOTTOS T., SMILANSKY U., Ann. Phys. (N.Y.), 274 (1999), 76.
[22] ALTSHULER B., AHARONOV A., SPIVAK B., Pisma Zh. Eksp. Teor. Fiz., 33 (1981), 101, (JETP Lett., 33, 94, (1981)).

Received 12 October 2004
Revised 25 October 2004